CHAPTER 4 EFFECT OF OPERATING TEMPERATURE, FLOWING ELECTROLYTE, MATERIALS, FREQUENCY AND DUTY CYCLE IN KOH

In the preceding chapters a relationship of the current density, temperature, bubble diameter, height of electrode, distance between electrodes, operating time and concentration of ions have discussed with the models of void fraction, conductivity and resistance. This chapter aims to study the effects of the alkaline electrolytic reaction on the gas production rate and efficiency via empirical method which are divided into four experiments as follows: 1) the effect of flowing electrolyte 2) the effect of solution temperature 3) the effect of electrode materials and 4) the effects of frequency and duty cycle.

4.1 Experimental Apparatus

The water electrolysis is conducted under atmospheric pressure using the pressure switch controller. The pressure switch (P) is connected to measure the gauge pressure of produced hydrogen and oxygen gases. Electrodes are rested on a support, grooved for keeping a fixed or varied distance between electrodes. AC power supply is connected to a bridge rectifier through a step down transformer (5.3 KVA, input: 220/230 V AC). The electrodes are connected with AC to DC converter. Regulated DC power supply working in the range of 10-160 A is used and the current is adjusted in the range of 5 - 60 A. Voltmeter (V) and ammeter (A) are connected in parallel and series respectively to the electrolyzer to measure voltage and current applied to electrolysis process. The gases obtained from the cathode and the anode are collected separately in gas tube and the volume of hydrogen and oxygen produced is measured with hydrogen digital gas mass flow meter and flow meter for oxygen and re-checked by water displacement. Temperature, voltage and current are recorded by the NI-USB6218 (DAQ) as illustrated in figure 4.1.

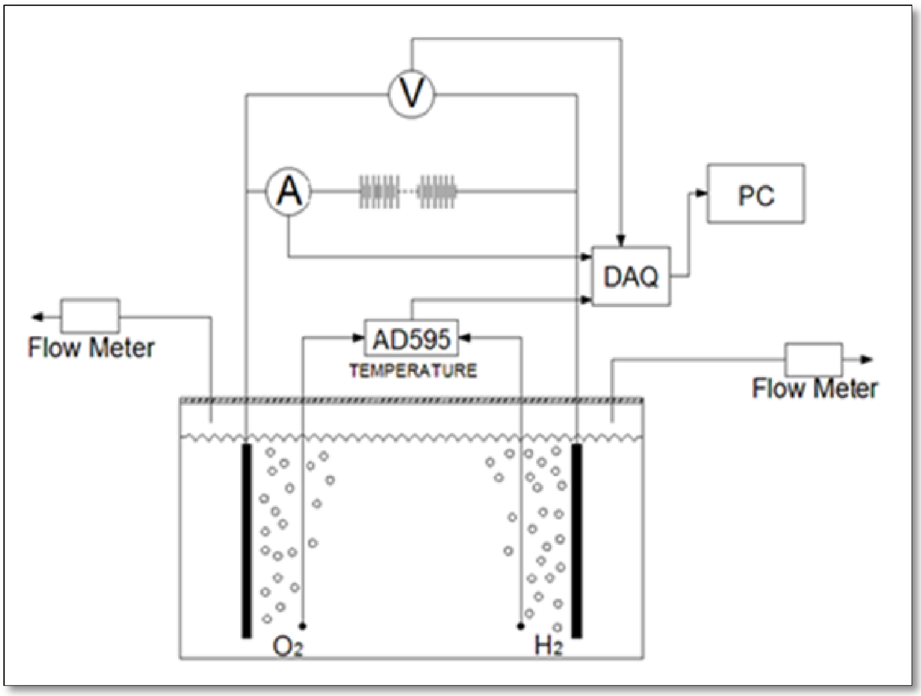

Figure 4.1 Diagram of experimental apparatus

4.2 Experimental Design

Response surface methodology or RSM is a collection of mathematical and statistical techniques that are useful for the modeling and analysis of a problem in which a response of interest is influenced by several variables and the objective is to optimize this response. The form of the relationship between the response (Y) and the factors (x_i) is given by Eq.4.1 which is called the second-order model. It is used for a polynomial of higher degree (Montgomery, 2001).

$$Y=\beta_0+\sum_{i=1}^{k}\beta_i x_i+\sum_{i=1}^{k}\beta_{ii}x_i^2+\sum_{i<j}\sum\beta_{ij}x_i x_j+\varepsilon \qquad (4.1)$$

where β_0 is the arithmetic mean value of the responses, β_i corresponds to the factor effects, β_{ii} is the quadratic effects and β_{ij} is the interactions between the various factors. The ε variable stands for the fitting error. Almost all RSM problems use one or both of these models. Of course, it is likely that a polynomial model will be a reasonable approximation of the true functional relationship over the entire space of the independent variables.

4.3 Experimental Setup

The materials and apparatus in this chapter are the same ones employed in Chapter 3.

In each experiment, preparations of the system are similar but experimental conditions are different.

4.3.1 The Effect of Flowing Electrolyte

The objective of this section is to improve the electrolyte conductivity by means of circulating the electrolyte solution through pumping and to study the amount of gas generated. The effect of circulation with pumping on the gas production will be investigated. In this study, current and electrolyzer are considered as input data and the gas production rate as output data (Y). The levels adopted for factors are summarized in table 4.1. The diagram of the experimental apparatus is shown in figure 4.2. There is also a study the effect of electrolyte circulation by pumping. However, the study did not focus on the amount of oxygen existing in the electrolyte solution.

Table 4.1 Parameters of flowing electrolyte

Factor	Number of Level	Value of Level
Current	5	10, 15, 20,25, 30 (A)
Circulation	2	with and without flowing
Pressure		Atmospheric
Electrodes	Material	alloy steel
Electrolyte	KOH	10% wt 95% purity

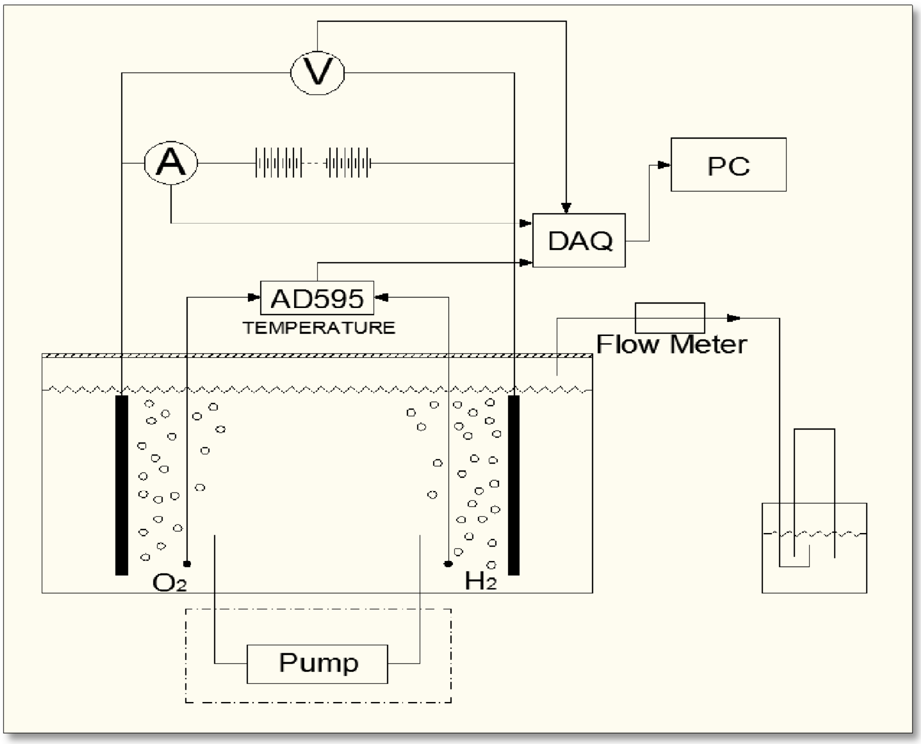

Figure 4.2 Diagram of experimental apparatus with pumping

4.3.2 The Effect of Solution Temperature

This section aims to the study effect of temperature on the hydrogen production rate from electrolysis process and include the efficiency of the system. The experiments are conducted at different solution temperature varying between 303 K and 353 K as exposed in table 4.2. The diagram of the experimental apparatus is shown in figure 4.1.

Table 4.2 Parameters of solution temperature

Factor	Number of Level	Value of Level
Current	6	10, 20, 30, 40, 50, 60 (A)
Solution temperature	6	303, 313, 323, 333, 343, 353 (K)
Pressure		Atmospheric
Electrodes	Material	alloy steel
	Distance between electrodes	X = 30 cm.
	Height	H = 10 cm.
	Width	W = 10 cm.
Electrolyte	KOH	20% wt

4.3.3 The Effects of Electrode Materials

This section investigates the effects of electrode materials and size of surface area on hydrogen production rate and efficiency in electrolytic process. The electrode materials are stainless steel, Cu, stainless steel+Ni with 20%wt KOH as exposed in table 4.3. The diagram of the experimental apparatus is shown in figure 4.1.

Table 4.3 Parameters of materials

Factor	Number of Level	Value of Level
Current	5	20, 30, 40, 50, 60 (A)
Material	3	stainless steel, Cu, stainless steel+Ni
Pressure		Atmospheric
Electrodes	Distance between electrodes	X = 30 cm.
	Height	H = 10 cm.
	Width	W = 10 cm.
Solution temperature		343 (K)
Electrolyte	KOH	20% wt

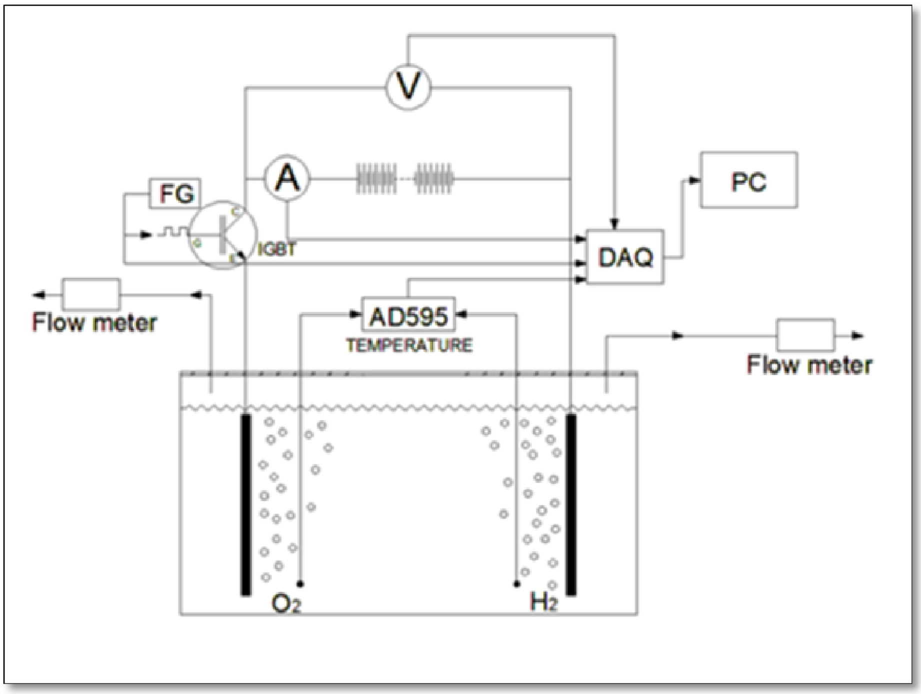

Figure 4.3 Diagram of experimental apparatus with function generator and IGBT

4.3.4 The Effects of Frequency and Duty Cycle

The diagram of the experimental apparatus in this section is shown in figure 4.3. Insulated Gate Bipolar Transistor (IGBT) is connected in series to the electrolyzer to control the voltage and the current supplied to the system. Function Generator (FG) working in the range of 20-80 % duty cycle and 0.1Hz - 4 MHz is used to adjust the duty cycle and frequency in the range of 20-80 % duty cycle and 0.1-100 Hz, respectively. Parameters varied are current, frequency and duty cycle as shown in table 4.4. The effects of frequency and duty cycle on the hydrogen production rate and efficiency will be investigated and the results will be subsequently discussed.

Table 4.4 Parameters of frequency and duty cycle

Factor	Number of Level	Value of Level
Current	4	30, 40, 50, 60 (A)
Frequency	7	0.1, 0.5, 1, 5, 10, 50, 100 (Hz)
Duty Cycle	3	20, 50, 80
Pressure		Atmospheric
Electrodes	Material	alloy steel
	Distance between electrodes	X = 20 cm.
	Height	H = 10 cm.
	Width	W = 10 cm.
Electrolyte	KOH	20% wt

For effect of current density, concentration and distance between electrodes in NaOH and NaCl as shown in Appendix B.

4.4 Results and Discussion

The results are consists of the analysis of correlation of parameters, in particular, the significance of the regression model obtained from the experimental data and the effect of temperature, flowing electrolyte, materials, frequency and duty cycle influencing on hydrogen production and improvement the electrolysis process. For the calculation of efficiency is shown appendix C.

4.4.1 Correlation between Current Density and Operating Temperature on Potential of electrolyzer and Hydrogen Production Rate

Figure 4.4 shows the estimation of regression coefficients, T-score and P-value between the potential of electrolyzer, and two important factors, including current density and operating temperature (solution temperature). The coefficient of factors taken into consideration is determined by the P-value which is less than the significance level of 0.05. Correlation of current density and operating temperature on potential of electrolyzer are shown in Eq. 4.2.

$$\mathrm{Y} = 128.125 - 0.693A - 0.013B + 0.001A^2 \tag{4.2}$$

where A is the temperature of the solution (K), B is the current density (mAcm-2), and Y is the potential (V).

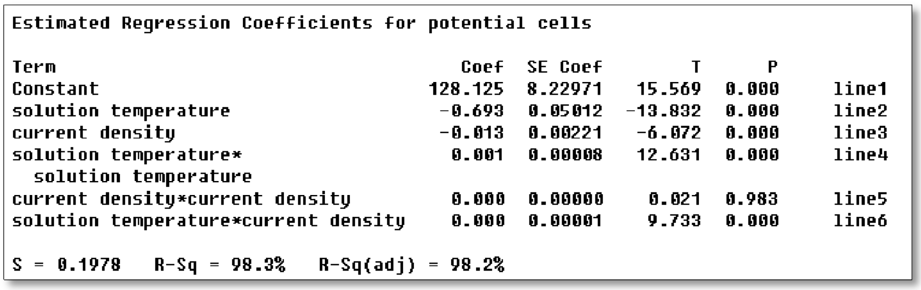

```
Estimated Regression Coefficients for potential cells

Term                                  Coef  SE Coef       T      P
Constant                           128.125  8.22971  15.569  0.000     line1
solution temperature                -0.693  0.05012 -13.832  0.000     line2
current density                     -0.013  0.00221  -6.072  0.000     line3
solution temperature*                0.001  0.00008  12.631  0.000     line4
  solution temperature
current density*current density      0.000  0.00000   0.021  0.983     line5
solution temperature*current density 0.000  0.00001   9.733  0.000     line6

S = 0.1978   R-Sq = 98.3%   R-Sq(adj) = 98.2%
```

Figure 4.4 The result of Response Surface Regression: Potential (V) versus Current density (Amm^{-2}) and Temperature (K)

The model of Eq.4.2 is suitable for calculating the optimal potential of electrolyzer and the coefficient R^2 and adj-R^2 equal to 98.3% and 98.2%, respectively. The level of the factors or the area in contour refers to the potential of electrolyzer that occurs when the current density and operating temperature are fixed. Figure 4.5 demonstrates the contour and optimum of potential. As indicated in figure 4.5, the solution temperature and current density condition have considerable influence on the extent of potential. Figure 4.5 indicates that the increasing solution temperature partially defers the potential. The temperature is part of the driving force for mass transfer in which the rise of temperature results in the increase of rate of reaction and the decrease of potential. The optimum of potential is less than 5 volts at solution temperature more than 330 K and the current density between 100 and 150 mAcm^{-2}, approximately.

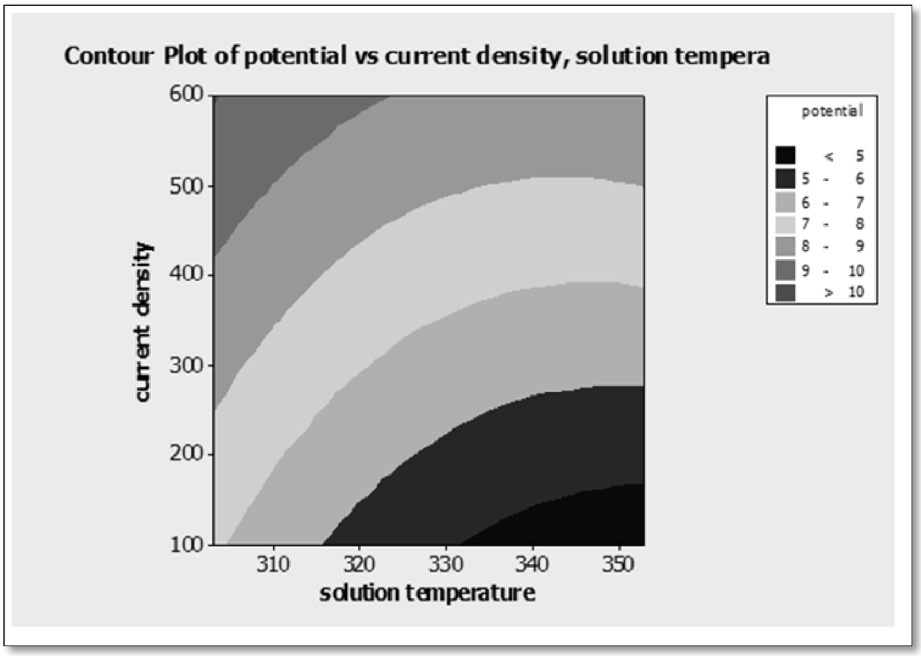

Figure 4.5 The contour plots of a response surface of potential (V)

Factors analysis of current density and operating temperature are exposed in figure 4.6. Figure 4.6 shows the estimation of regression coefficients, T-score and P-value between the hydrogen production rate, and three important factors, including current density and operating temperature. The coefficient of factors taken into consideration is determined by the P-value which is less than the significance level of 0.05.

Relationship of current density and operating temperature on the hydrogen production rate are shown in Eq. 4.3.

$$\mathrm{Y} = -4.96698 + 0.02949A - 0.00301B - 0.00004A^2 + 0.00001AB \qquad (4.3)$$

where A is the temperature of the solution (K), B is the current density (mAcm^{-2}), and Y is the hydrogen production rate (Lmin^{-1}). The model of Eq.4.3 is suitable for calculating the optimal hydrogen production rate and the coefficient R^2 and adj-R^2 equal to 99.1% and 99.1%, respectively.

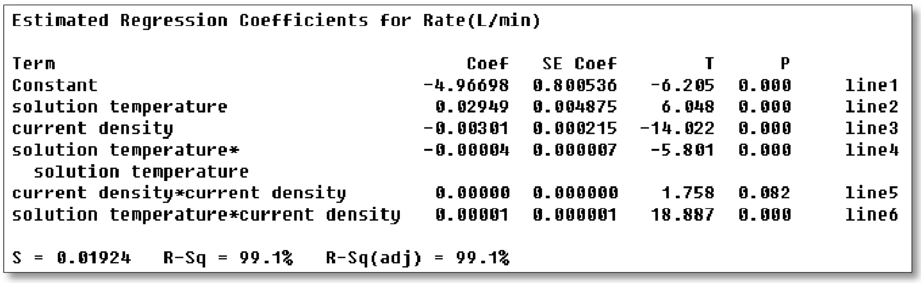

```
Estimated Regression Coefficients for Rate(L/min)

Term                                     Coef  SE Coef       T      P
Constant                             -4.96698 0.800536  -6.205  0.000     line1
solution temperature                  0.02949 0.004875   6.048  0.000     line2
current density                      -0.00301 0.000215 -14.022  0.000     line3
solution temperature*                -0.00004 0.000007  -5.801  0.000     line4
  solution temperature
current density*current density       0.00000 0.000000   1.758  0.082     line5
solution temperature*current density  0.00001 0.000001  18.887  0.000     line6

S = 0.01924   R-Sq = 99.1%   R-Sq(adj) = 99.1%
```

Figure 4.6 The result of Response Surface Regression: Rate ($Lmin^{-1}$) versus Current density (Amm^{-2}) and Temperature (K)

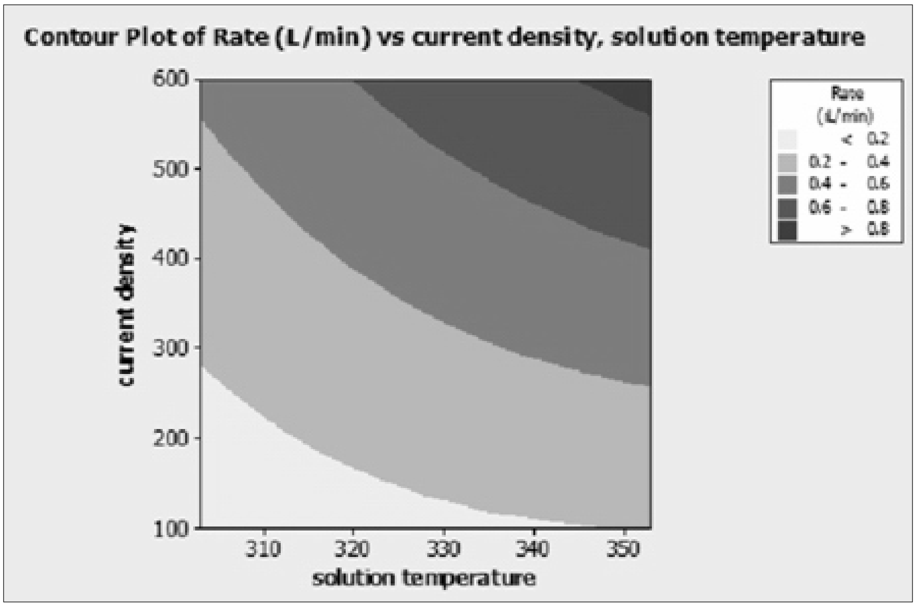

Figure 4.7 The contour of a response surface of gas production rate ($Lmin^{-1}$)

Figure 4.7 presents contour plots indicating the effect of solution temperature and current density on hydrogen production rate under the predefined conditions. As indicated in figure 4.7, the maximum hydrogen production rate of 0.8 $Lmin^{-1}$ is occurred at 600 $mAcm^2$ and at 350 K. Besides higher temperature resulting in a potential drop is also involved in the catalytic reaction. Eqs. 4.2 and 4.3 can be used to determine the relationship between the current density and temperature on the potential of electrolyte and the hydrogen production rate, respectively.

4.4.2 The Effect of Frequency and Duty Cycle

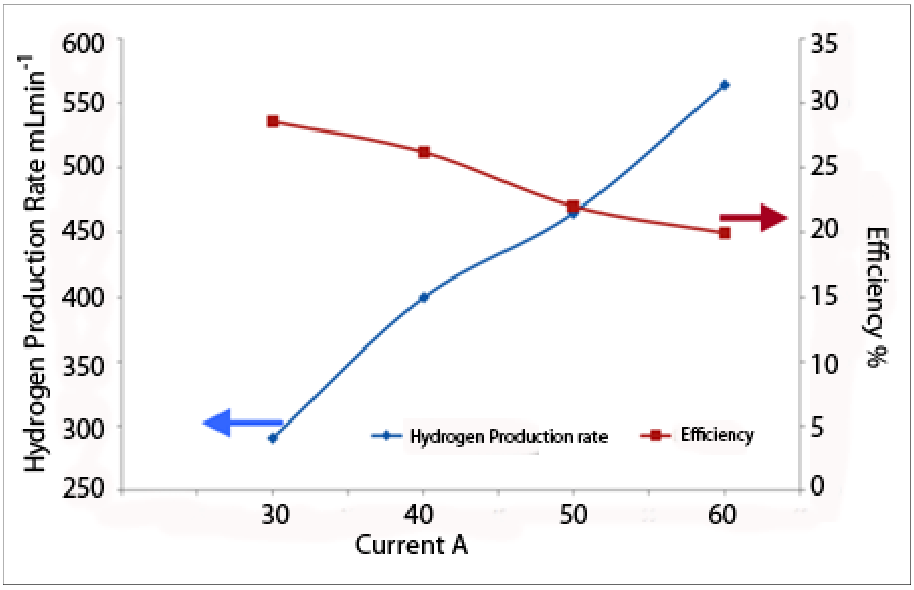

Figure 4.8 Effect of Direct Current on hydrogen production rate and efficiency

Figure 4.8 shows the hydrogen production rate (mLmin^{-1}) and the efficiency of the electrolysis process. The experimental data show that the hydrogen production rates varies from 290 mLmin^{-1} at 30 A to 564 mLmin^{-1} at 60 A. However, the efficiency of electrolyzer is varied from 28.57 % at 30 A to 19.98 % at 60 A, respectively. This is because the higher amount of bubble that occurs in the electrolyte by increasing the current inhibits the movement of electrons that flow from the power supply. Consequently, the increase of bubble volume leads to a decrease of conductivity of electrolyte at which its contamination is high.

From characteristics of direct current to influence the rate and efficiency of gas as mentioned above which consider that it is clearly observed that as the direct current is increased, the hydrogen production rate is also increased due to the additional quantity of charges in the reaction. Figure 4.9illustrates hydrogen production rate at different duty cycles where the DC distributions are controlled by PWM of 1-100 Hz and 20, 50 and 80 % duty cycle. From figures 4.9a, 4.9b and 4.9c, it has been found that when the duty cycle is enlarged, hydrogen production rate is augmented due to the fact that higher duty cycle has the longer time interval of supplying power resulting in the longer transfer of electrons at the interface between the surface electrode and electrolyte. At the same duty cycle, gas production rate is enhancing with a lessening of frequency because the effect of impedance caused by the electrolyte resistance and capacitance varies with the frequency of the current passing through the circuit. At each duty cycle of 1 Hz, it can be observed that hydrogen gas can be produced at maximum rate.

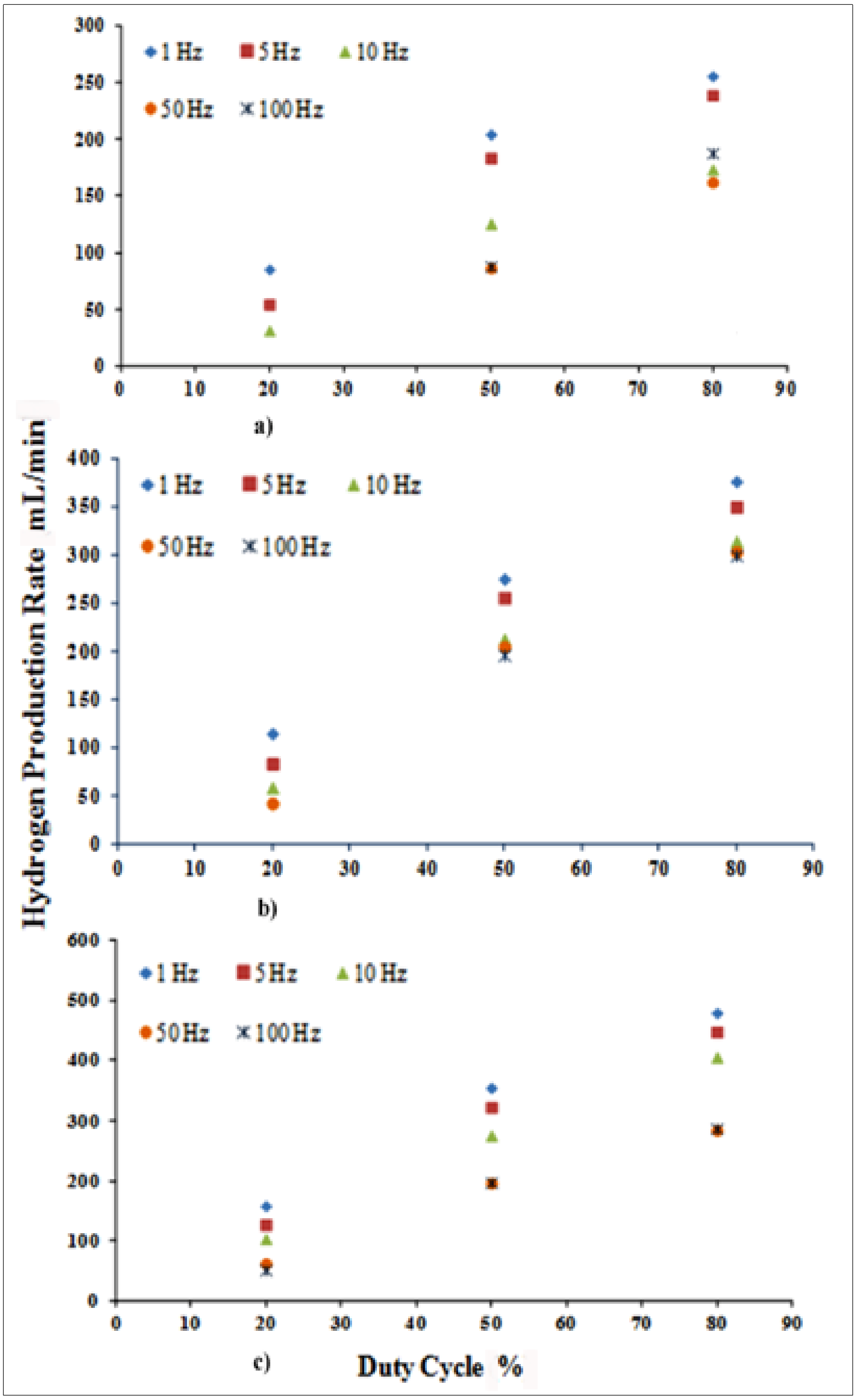

Figure 4.9 Effect of duty cycle on hydrogen production rate a) 30 A, b) 40 A and c) 50A

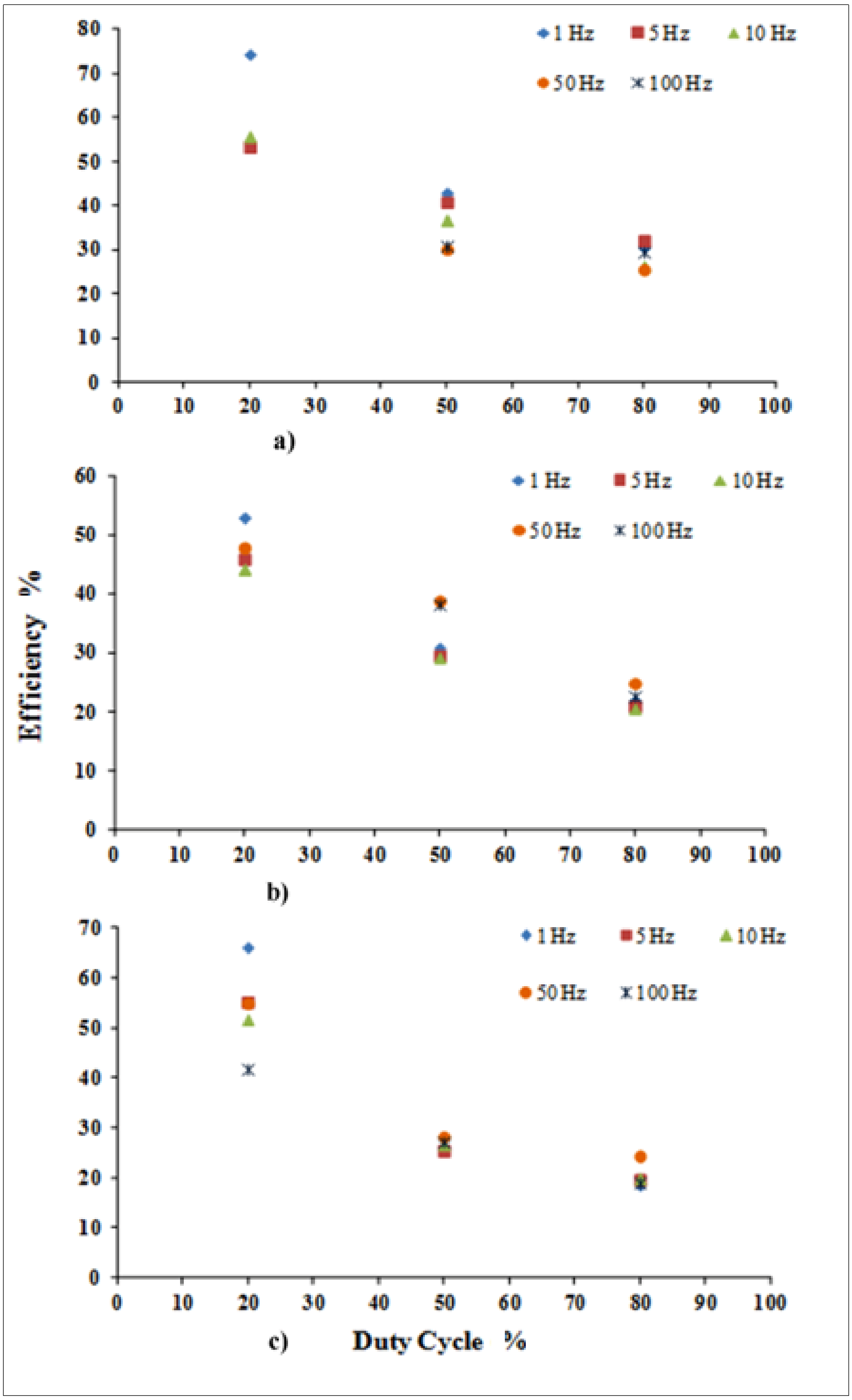

Figure 4.10 Effect of duty cycle on efficiency a) 30 A, b) 40 A and c) 50 A

Figures 4.10a, 4.10b and 4.10c show the effect of duty cycle on the efficiency at the current of 30, 40 and 50 Amps, respectively. At the frequency of 1 Hz, the efficiency is highest due to the small amount of gas bubbles is occurred on the electrode and slightly blocked the electrical current flow. From the study, it can be determined that the duty cycle has an influence on the efficiency at which 20 % duty cycle has higher efficiency than those at 80 % duty cycle since the higher duty cycle allows longer time-on period than the time-off period. Therefore, more current flows into the system, leading to higher amount of hydrogen. On the other hand, when the gas production is increased because power input is increased in the system, the efficiency is directly affected where the efficiency is decreased as the duty cycle is risen. This is due to the fact that an increase of duty cycle results in the higher power input and a number of bubbles to the electrolyte, leading to the higher resistance.

Comparisons of the rate of hydrogen production between the continuous DC power supply and pulsating DC power supply at various duty cycles are shown in figure 4.11. From figures 4.11a, 4.11b and 4.11c, it can be observed that, for the pulsating DC power supply, the hydrogen production rate is reduced with an increase of frequency. This is because the time interval of turning the circuit on and off is brief so the small quantity of power is consumed. Higher frequency has an effect on a decrease of average current, leading to a reduction of electrons in the reaction. At the same frequency, the rate of hydrogen production is increased when the duty cycle is increased because a rise of supplied current causes the higher amount of the electrons resulting in the higher rate of hydrogen production. This suggests that at the current of 30 A in figure 4.11a with an output pulse at frequency of 1, 5, 10, 50 and 100 Hz, hydrogen cannot be produced more than that of the continuous DC electrical power since the power of pulsating input to the system is less than the continuous DC power supply. It can be seen in figures 4.11b and 4.11c that, with the frequency of 1-5 Hz and the duty cycle of 80 %, hydrogen gas production rate is closed to that of the continuous DC power supply since electrons of continuous direct current into the reaction with a combination at electrode surface layers resulting in the bubble layer remaining in the electrolyte. For the PWM, the reaction is a break periodically resulting gas not impedes the reaction to occur. In figure 4.11c, it can be observed that the hydrogen production rate at every duty cycle is likely to decrease when frequency is increased. At the same frequency, the rate of hydrogen production is increased when duty cycle is risen with the same reasons described in figures 4.11a and 4.11b. For current at 50 A in figure 4.11c, it can be found that, at the frequency of 1 Hz and 80% of duty cycle, hydrogen production rate is equal to that of the continuous DC power supply.

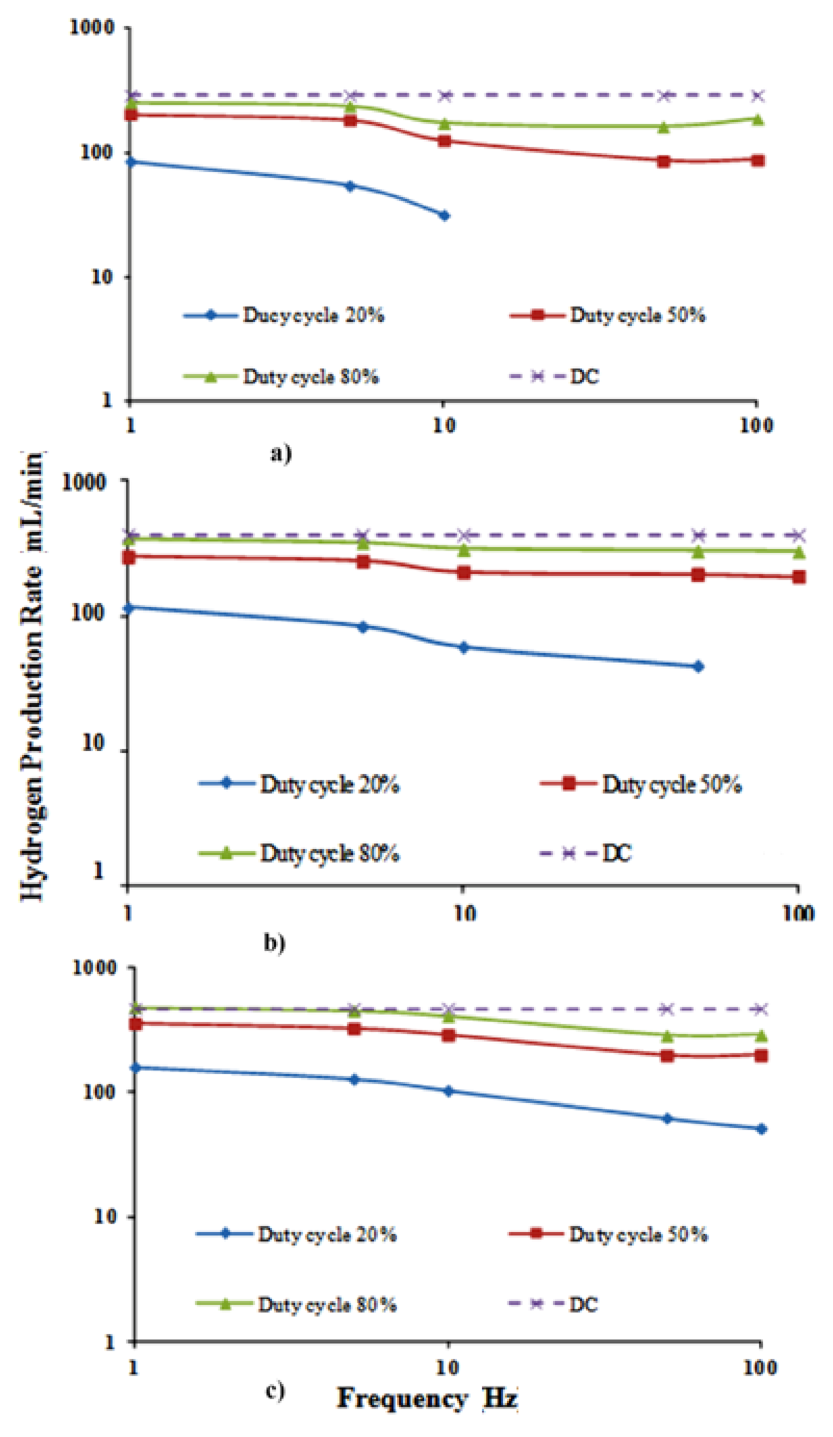

Figure 4.11 Effect of frequency on hydrogen production rate a) 30 A, b) 40 A and c) 50 A

From the study, it can be explained that when the frequency enlarges, hydrogen production rate is lessened in view of the fact that less current flows into the system, making the current density diminish and the power input to the system reduce. The frequency is increased resulting in a decline of efficiency. Brisse et al. (2008) is reported the impedance decreases strongly with increasing temperature and the ohmic impedance value at low frequency. From figures 4.10 and 4.11, it has been found that, frequency has an influence on the lower duty cycle than the higher duty cycle because the time interval of turning on and turning off of the system affect the current distribution, amount of current and reaction rate.

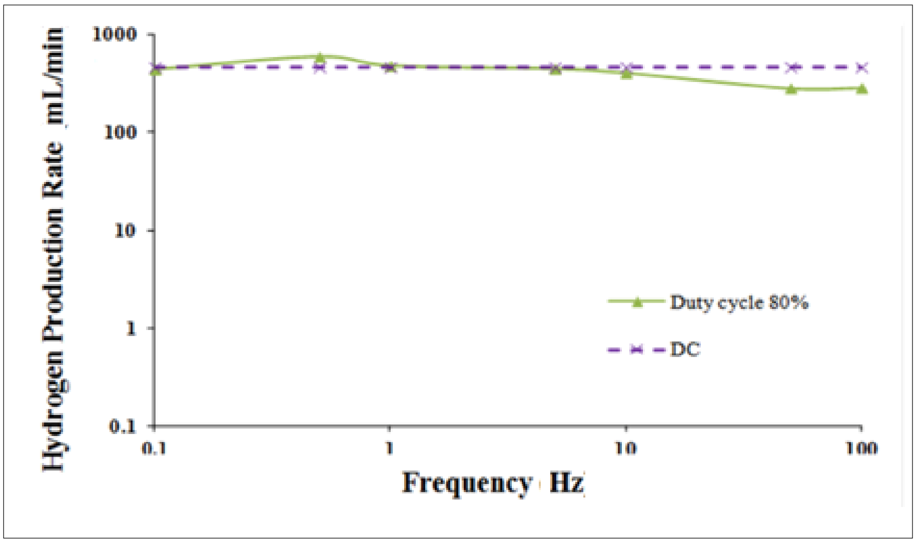

Figure 4.12 Effect of frequency on hydrogen production rate at 50 A

Figure 4.12 presents the hydrogen production rate at the frequencies of 0.1 Hz, 0.5 Hz and continuous DC power. It has been found that at lower than 5 Hz of frequency, hydrogen production rate of pulse is higher than that of the DC power supply. Therefore, if the equal amount of energy is input to the system at 20% duty cycle, the hydrogen production rate is at its highest at the low frequency. Furthermore, the pulsating DC power supply can solve the problem of accumulation of the ions at the electrode surface. This is because during the time-off period, reactions are terminated without ion movement at the electrode surface.

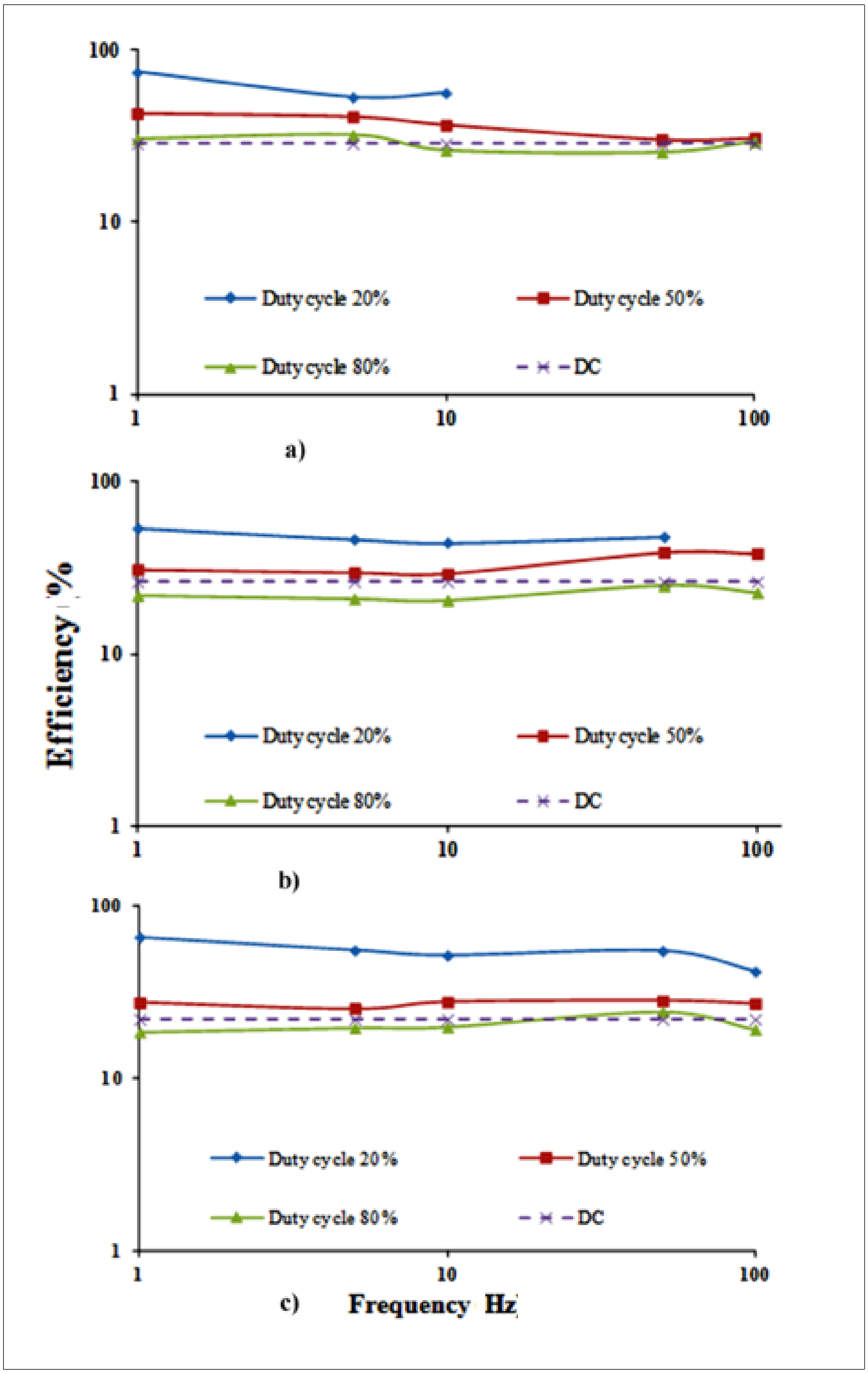

Figure 4.13 Effect of frequency on efficiency a) 30 A, b) 40 A and c) 50 A

Figure 4.13 shows the comparison of the efficiency of the electrolysis process between the continuous DC power supply and pulsating DC power supply at various duty cycles. It can be observed that the efficiency of the system is lessening with an increase of frequency since there are gas bubbles growing at the electrodes. For every duty cycle at 30 amperes in figure 4.13a, at the frequency of 1-5 Hz, the system with power control using pulse is more efficient than DC one. At the current of 40 and 50 amperes in figures 4.13b and 4.13c, it is found that only the efficiency of 80 % duty cycle is lower than the DC one. While the efficiency of 20 % duty cycle for every frequency is greater than the efficiency of DC since the rate of electrochemical reaction is dependent on the electromotive force and the amount of current flowing into the system, so the bubbles cannot be ventilated instantly in which electrolyte containing gas bubbles causes the decrease of the conductivity and the efficiency. Figure 4.13 show that the increase of duty cycle and frequency makes the efficiency decrease.

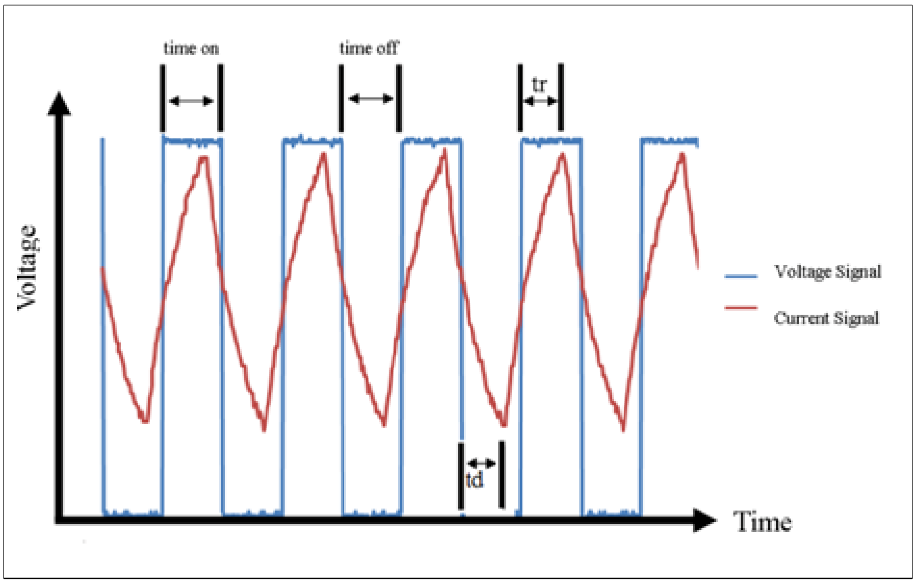

Figure 4.14 Voltage and current signal of experiment

The duty cycle of signal measures the fraction of time a given transmitter is transmitting that signal. This fraction of time determines the overall power delivered by the signal. Signals with longer duty cycle carry more power and require less efficient receivers than do signals with shorter duty cycles. Figure 4.14 demonstrates the voltage and current signal of experiment and figure 4.15 depicts the switching behavior of the process which has been carried out under inductive load obtaining both the turn off and reverses recovery waveforms.

The characteristic is the variation of the electric current flowing through the current of capacitive load. It has been found that when the voltage is turned off, current is reduced and current is boosted, the voltage is turned on. If $time_{off} \leq time_d$, complete loss phenomenon is occurred, else if $time_{off} > time_d$, a non complete loss due to the phenomenon still exists in the discharge of the load. Furthermore, non complete loss is easily occurred when duty cycle is highly adjusted because time$_{off}$ is reduced and the current cannot flow down to zero in time and remains outstanding. It is clearly observed that when the duty cycle is increased, the pulse is also increased due to the increase in the on-time pulse as there is no change in current and electrolyte conductivity, and the voltage remains fixed for all pulse signals according to Ohm's law.

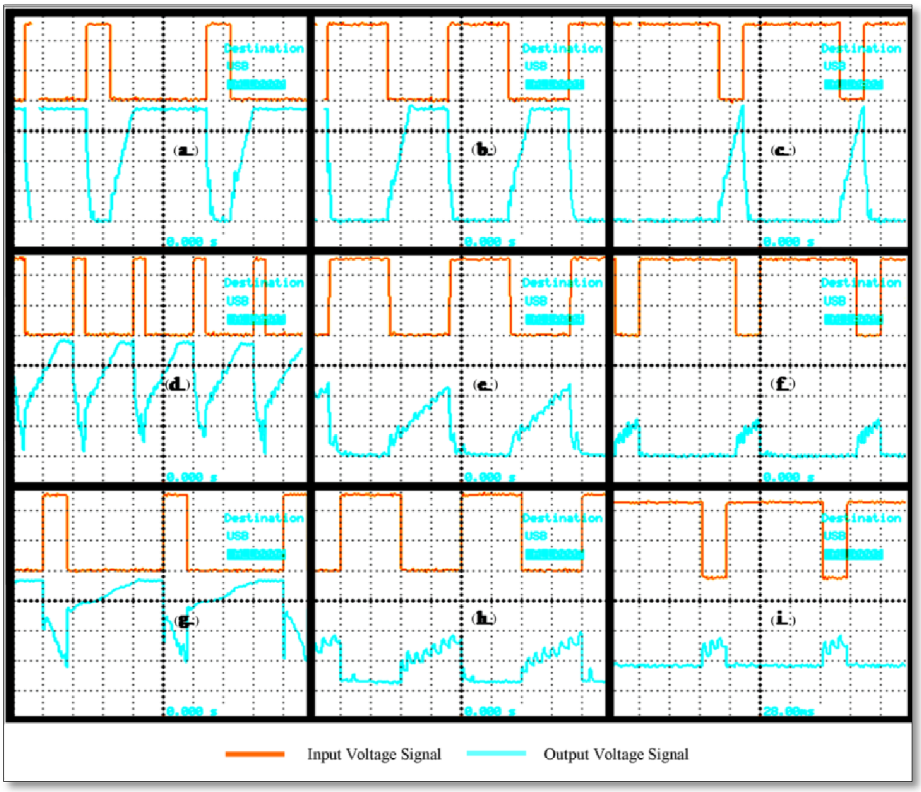

Figure 4.15 Wave forms of IGBT gate voltage and output voltage a) 20 % duty cycle 1 Hz, b) 50 % duty cycle 1 Hz, c) 80 % duty cycle 1 Hz, d) 20 % duty cycle 5 Hz, e) 50 % duty cycle 5 Hz, f) 80 % duty cycle 5 Hz, g) 20 % duty cycle 10 Hz, h) 50 % duty cycle 10 Hz and i) 80 % duty cycle 10 Hz

From the behavior of the pulse in the process, the polarization has changed due to the fact that the accumulation of gas bubbles is occurred on the electrodes and blocked the flow of electrical current. The reaction mechanism is formed by the characteristics of the voltage and current supplied to the electrolyzer. Power swings can cause the load impedance, which under steady state conditions is not within the IGBT's operating characteristic, to enter into the IGBT's operating characteristic. When impedance due to power swing matches with the operating impedance of the IGBT, it gives false tripping.

4.4.3 The Effect of Temperature

Figure 4.16 shows the potential of electrolyzer against the current density at different operation temperature. The potential is decreased when the system temperature is increased at every current density. The power consumption is calculated and plotted in figure 4.17. As can be seen from 4.16 and 4.17, the potential varies from 4.41 V at 100 mA/cm^2, 353 K to 10.14 V at 600 mA/cm^2, 303 K and the power consumption varies from 44.10W at 100 mA/cm^2, 353 K to 608.40 W at 600 mA/cm^2, 303 K, respectively. This is because the operating temperature has an effect on the diffusion coefficients of H^+ and O^{2-} ions which are higher at high temperature. It implies that H^+ and O^{2-} ions at high temperature have ability to move better than those at low temperature. Therefore, the electrical conductivity of the electrolyte solution is increased when the temperature is increased. These results agree well with the work done by Nagai et al. (2003) and Boll et al. (2003) who reported that the higher system temperature could cause the decrease of potential. This is also supported by the work of Roy et al. (2006) and Dieguez et al. (2008) who found that an increase of temperature had a direct effect on the voltage change according to Ohm's law. However, it is noted that when the temperature is raised, more steam is generated from the electrolyte, making the alkaline electrolyte solution more concentrated and hydrogen gas is mixed with more steam. Inevitably, steam in the gas mixture must be removed in order to obtain the rich hydrogen gas.

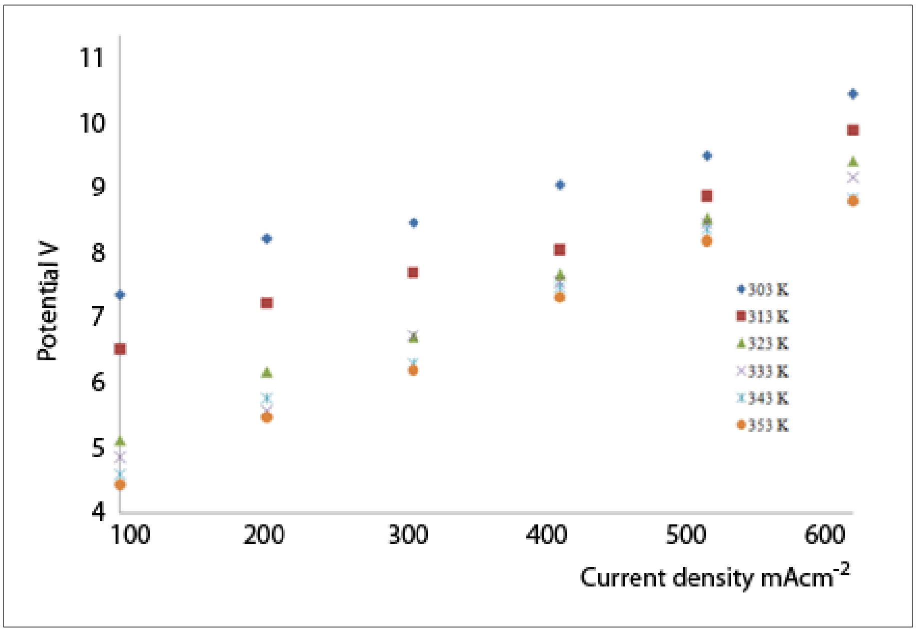

Figure 4.16 Correlation of current density and potential

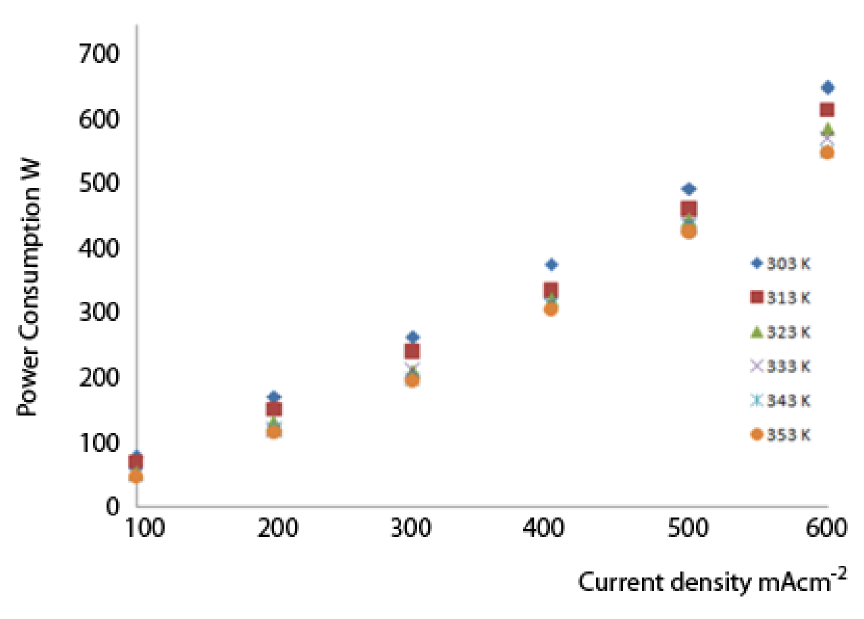

Figure 4.17 Relationship between power consumption and current density

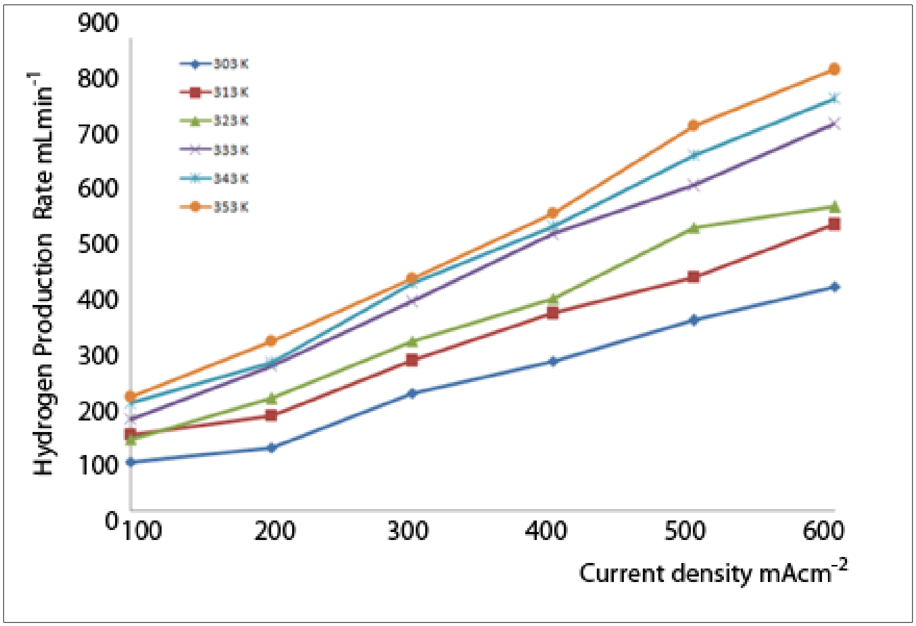

Figure 4.18 Tenor of hydrogen production rate at varying temperature

The experimental results of the operating temperature affect the rate of hydrogen gas production is illustrated in figure 4.18. In figure 4.18, the current density is plotted against the hydrogen production rate at different operating temperature, indicating that the higher current density yields the greater rate of hydrogen gas production. It can be seen that current density increases with the increasing rate of gas production which varies from 93 mLmin^{-1} at 100 mAcm^{-2}, 303 K to 840 mLmin^{-1} at 600 mAcm^{-2}, 353 K.

Theoretically, it is because the larger amounts of electrons enter to the system, thus high amount of gas is produced. Figure 4.19 describes the hydrogen production rate against the time of operation. This can be considered that hydrogen production rate does not change with a change of operating time and the hydrogen production rate is in the range between 800 and 900 mLmin^{-1}.

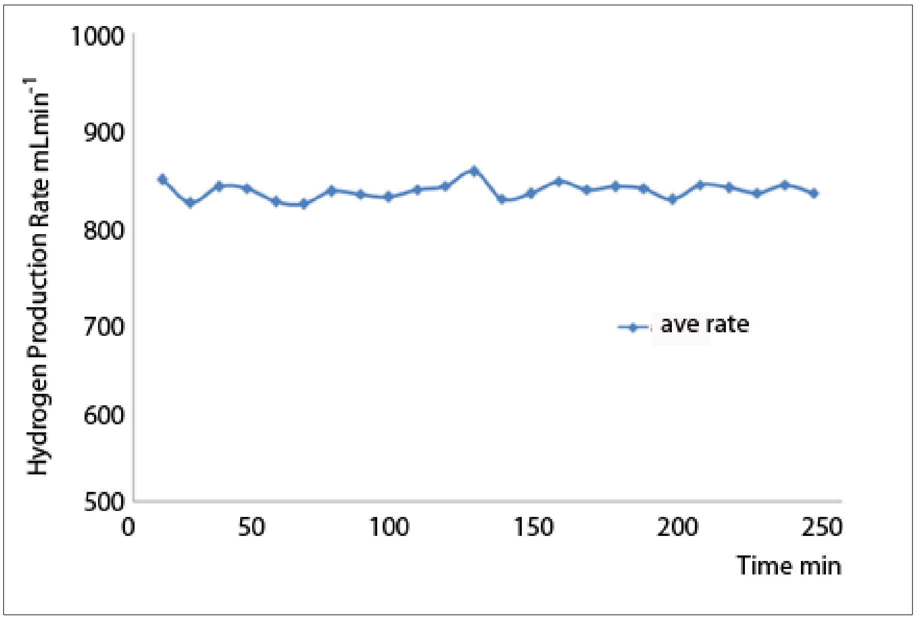

Figure 4.19 Relationship between operating time and hydrogen production rate

Figures 4.20 and 4.21 illustrate the plot of hydrogen production rate against the system temperature of copper and stainless steel, respectively. In this study, it can be observed that with the copper electrode the flow rate does not change with a variation of temperature. On the contrary, with the electrodes made of stainless steel, temperature affects the rate of hydrogen production. It is due to the fact that oxidation reaction is occurred at the surface of copper, while the film of chromium oxide is formed at the stainless steel surface to protect corrosion and electrode from chemical reduction. Therefore, the operating temperature should be also considered in the selection of electrode materials because it can help to increase the rate of gas production. However, lifetime of materials should be concerned for the study.

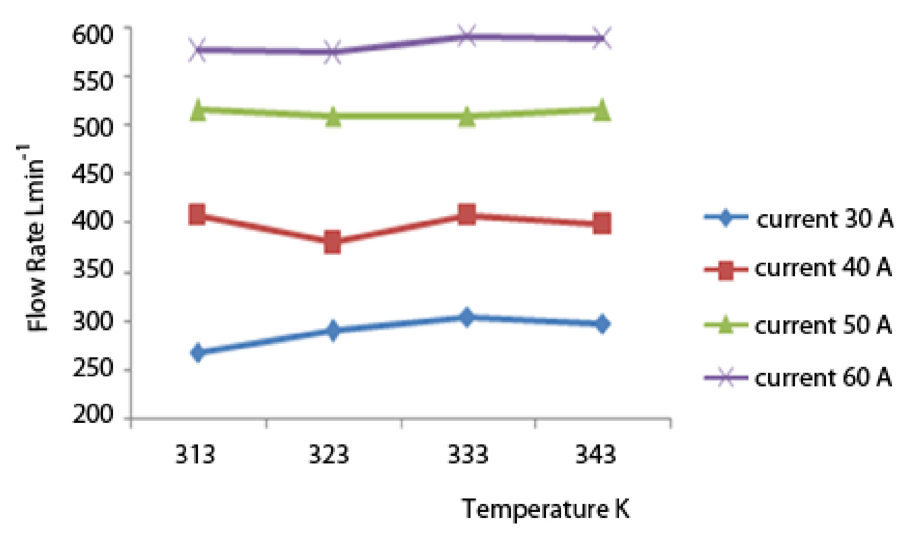

Figure 4.20 Effect of temperature on hydrogen production rate of copper

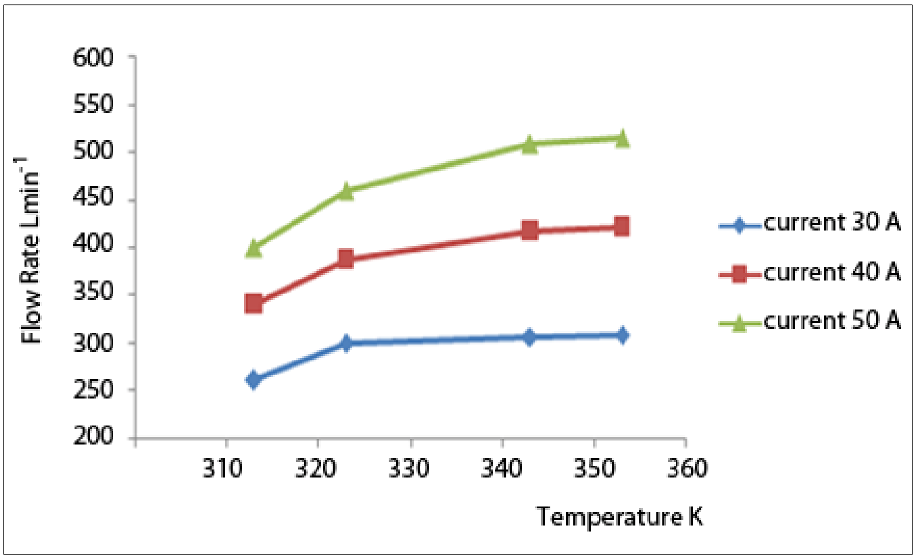

Figure 4.21 Effect of temperature on hydrogen production rate of stainless steel

4.4.4 The Effect of Materials

Figure 4.22 shows the relationship between the current density and the potential of electrolyzer among three different electrodes made of copper (Cu), stainless steel (SS) and nickel coated stainless steel. It has been found that the potential of copper electrode is higher than the potential of stainless steel and stainless steel covered with nickel, respectively. This is due to activities of ions in equilibrium with a given metal as show in table A.1. The hydrogen production rate is shown in Figure 4.23. As can be investigated, the hydrogen production rates of copper vary from 279 mLmin^{-1} at 200 mAcm^{-2} to 684 mLmin^{-1} at 600 mAcm^{-2} and the hydrogen production rates of stainless steel vary from 290 mLmin^{-1} at 200 mAcm^{-2} to 703 mLmin^{-1} at 600 mAcm^{-2} when the hydrogen production rates of stainless steel coated with nickel vary from 301 mLmin^{-1} at 200 mAcm^{-2} to 818 mLmin^{-1} at 600 mAcm^{-2}.

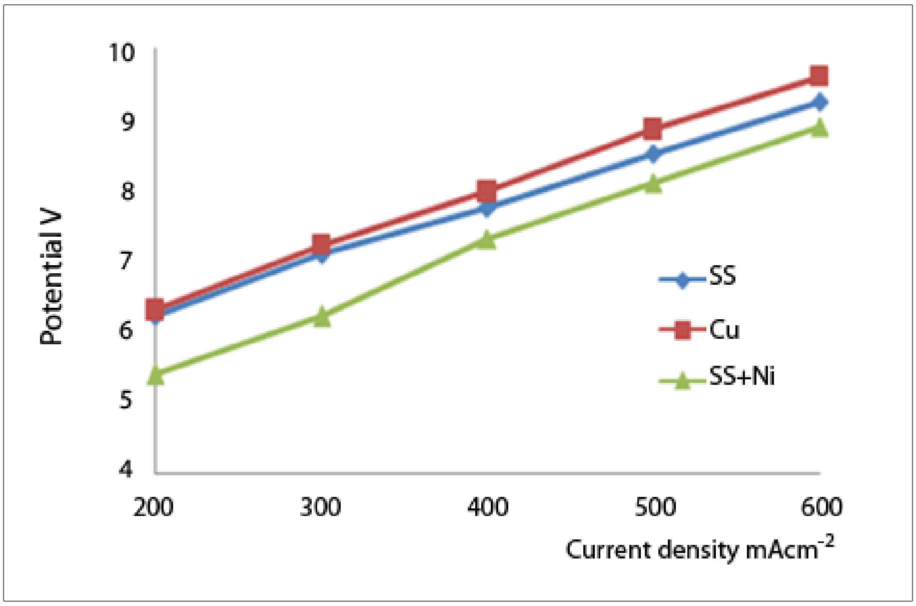

Figure 4.22 Relation of potential and current density

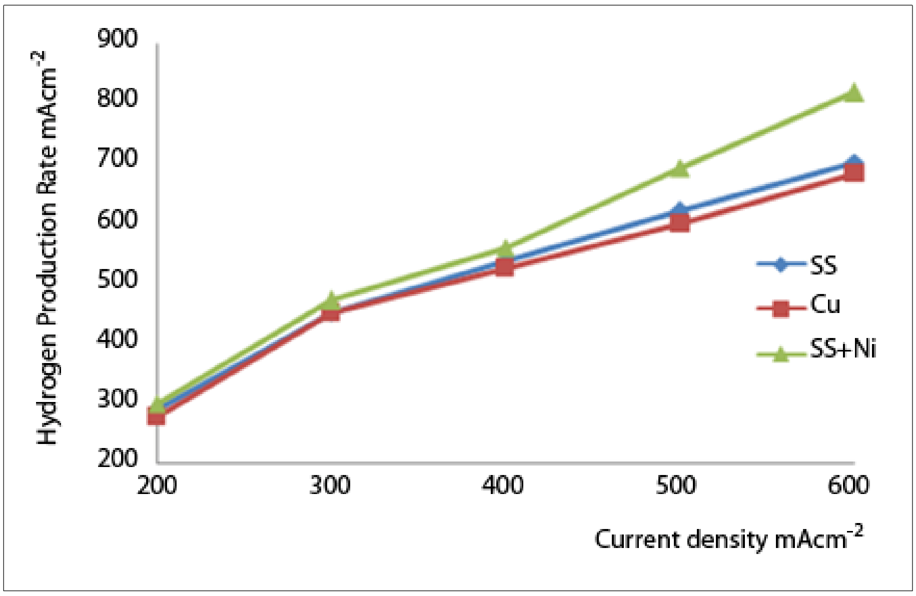

Figure 4.23 Difference of electrode materials on hydrogen production rate

Figure 4.23 shows that stainless steel covered with nickel is the highest hydrogen production rate and followed by stainless steel and copper, respectively. It is found that there is not much different in the hydrogen production rate of stainless steel and copper is not much different at all temperatures, while stainless steel covered with nickel has a higher production rate at higher temperature because the activation energy is less, the molecules will reach the transition stage early as it has to absorb less energy.

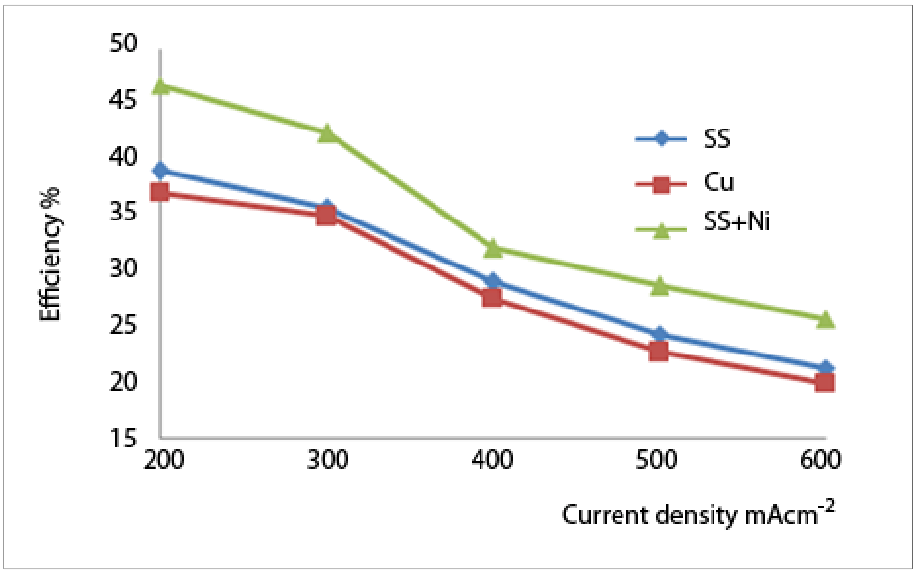

Figure 4.24 Difference of electrode materials on efficiency

Generally, the higher current density causes the increase of electrolyzer potential and the increase of hydrogen production rate. From figure 4.24, it is found that using a stainless steel coated with nickel electrodes can improve the efficiency of the system better than the use of iron and copper. Upon the increase of current density, it is found that the potential is developed as a result of the over-voltage on the surface electrodes occurred by the large quantity of gases covering the electrode surface, resulting in the difficult movement of ions.

4.4.5 The Effect of Flowing Electrolyte

The experimental results of the factors affecting the gas production rate are illustrated in figures 4.25 and 4.26. The difference between the gas production rate without pumping and the one with pumping are shown in figure 4.25. As can be seen, the gas production rates vary from 0.86 Lmin^{-1} at 10 A to 1.76 Lmin^{-1} at 30 A when the electrolyzer is operated without pumping, while the gas production rates are much higher in case of pumping, varying from 0.92 Lmin^{-1} at 10 A to 2.31 Lmin^{-1} at 30 A. In fact, the difference of gas production rate is caused by the conductivity of electrolyte solution. In the case without pumping, the conductivity was not consistent since the gas bubble occurs at the electrode surface. As a result, the electrical resistance of the electrolyte solution is higher and the conductivity of the electrolyte is decreased. In case of circulation with pumping, the bubble is dispersed throughout the electrolyte in which the bubble layer thickness on the electrode surface is lower, so the conductivity of the electrolyte is raised significantly especially at higher current.

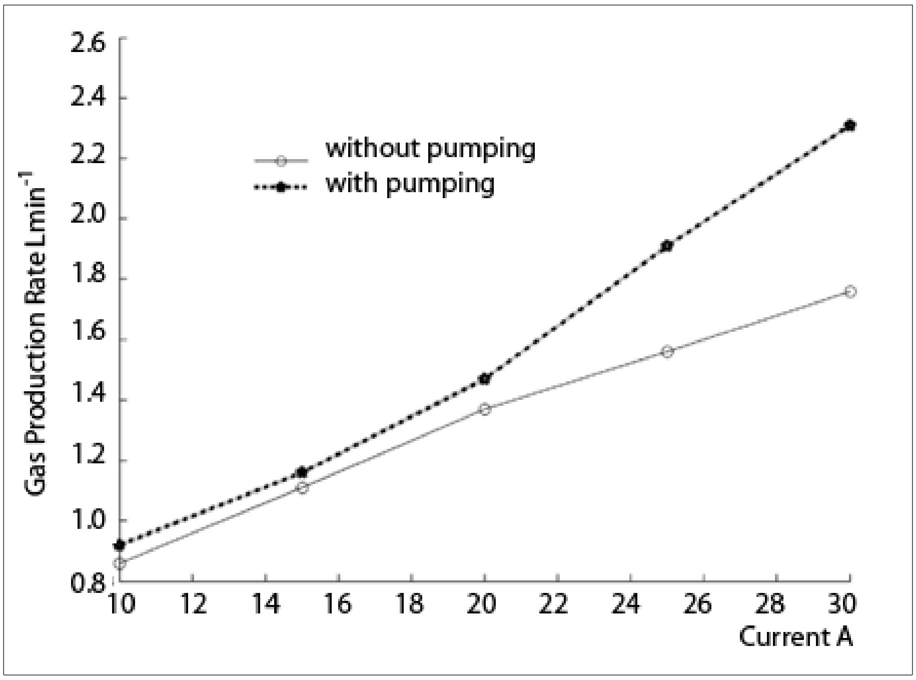

Figure 4.25 Current - gas production rate comparison of various pumping

Figure 4.25 also shows the gas production rate as different power consumption of the electrolyzer operation with and without pumping. It can be noted that the gas production rate ranges from 0.92 Lmin^{-1} at 106 watt (10 A) to 2.32 Lmin^{-1} at 520 watt (30 A) of circulation with pumping and, in the case without pumping, the gas production rate ranges from 0.86 Lmin^{-1} at 112 watt (10 A) to 1.76 Lmin^{-1} at 408 watt (30 A). These results express that, at the same power, the circulation with pumping produces higher gas volume than that of the circulation without pumping.

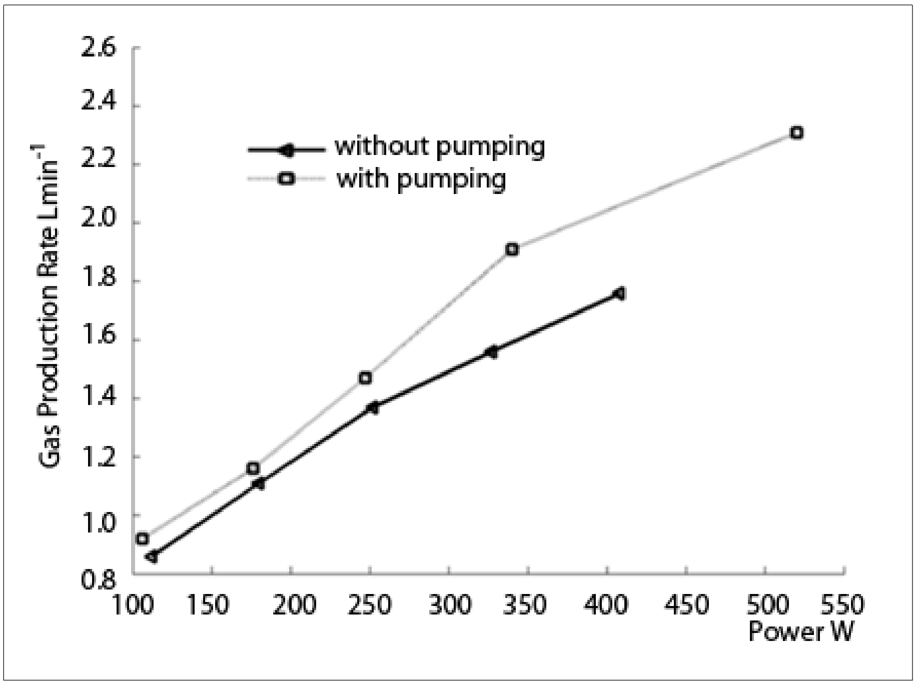

Figure 4.26 Power consumption - gas production rate comparisons of various circulation

From figures 4.25 and 4.26, the gas production rate is proportional to the amount of the current (electrons) applied. In addition, when the current is increased, the gas production rate without pumping is lower than the gas production rate of circulation with pumping because the accumulation of gas bubbles is occurred on the electrode surface, thereby blocking the flow of electrical current. Sarkar et al. (2010) reported that gas produced at the electrode and dissolved directly into the liquid would diffuse in to the rising bubble. Therefore, the bubble layer could cause a change in conductivity than those larger bubbles.

4.4.6 Correlation between Current Density, Operating Temperature Frequency, Duty Cycle and %wt on Hydrogen Production Rate

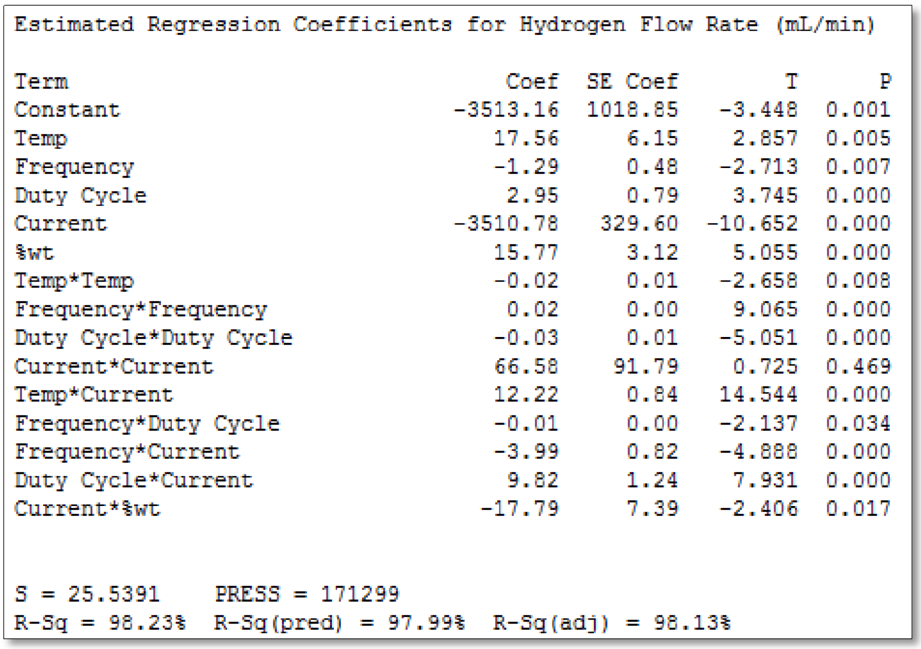

```
Estimated Regression Coefficients for Hydrogen Flow Rate (mL/min)

Term                                Coef  SE Coef        T      P
Constant                        -3513.16  1018.85   -3.448  0.001
Temp                               17.56     6.15    2.857  0.005
Frequency                          -1.29     0.48   -2.713  0.007
Duty Cycle                          2.95     0.79    3.745  0.000
Current                         -3510.78   329.60  -10.652  0.000
%wt                                15.77     3.12    5.055  0.000
Temp*Temp                          -0.02     0.01   -2.658  0.008
Frequency*Frequency                 0.02     0.00    9.065  0.000
Duty Cycle*Duty Cycle              -0.03     0.01   -5.051  0.000
Current*Current                    66.58    91.79    0.725  0.469
Temp*Current                       12.22     0.84   14.544  0.000
Frequency*Duty Cycle               -0.01     0.00   -2.137  0.034
Frequency*Current                  -3.99     0.82   -4.888  0.000
Duty Cycle*Current                  9.82     1.24    7.931  0.000
Current*%wt                       -17.79     7.39   -2.406  0.017


S = 25.5391    PRESS = 171299
R-Sq = 98.23%  R-Sq(pred) = 97.99%  R-Sq(adj) = 98.13%
```

Figure 4.27 The result of Response Surface Regression: Rate ($Lmin^{-1}$) versus Current density (Amm^{-2}), Temperature (K), Frequency (Hz), Duty Cycle and %wt ($moll^{-1}$)

The results consists of the analysis of correlation of parameters, in particular, the significance of the regression model obtained from the experimental data and the effect of direct current, concentration, temperature, frequency and duty cycle influencing on the hydrogen production and the improvement of the electrolysis process. The results of statistical calculations show that the significant changes of parameters give insignificant values of the hydrogen production rate as shown in figure 4.27 with significant level at 0.05. As a consequence, this can be used to improve the design of the electrolyzer and to maintain the electrolyte with the high conductivity. Figure 4.27 shows the estimation of regression coefficients, T-score and P-value between the hydrogen production rate, and three important factors, including current density, concentration, distance between electrodes and others. The coefficient of factors taken into consideration is determined by the P-value which is less than the significance level of 0.05. Correlation of current density, operating temperature, frequency, duty cycle and %wt on Hydrogen Production Rate are shown in Eq. 4.4.

$$\begin{aligned} \mathrm{Y} \; = \; & -3513.16 + 17.56A - 1.29B + 2.95C - 3510.78D \\ & + 15.77E - 0.02A^2 + 0.02B^2 - 0.03C^2 + 66.58D^2 + 12.22AD \\ & - 0.01BC - 3.99BD + 9.82CD - 17.79DE \end{aligned} \tag{4.4}$$

where A is the temperature of the solution (K), B is the frequency (Hz), C is the duty cycle, D is the current density ($\mathrm{Acm^{-2}}$), E is the %wt, and Y is the hydrogen production rate ($\mathrm{mLmin^{-1}}$).

4.5 Summary

For the temperature, it has been found that the hydrogen production rate and efficiency are increased at higher temperature. Efficiency is inversely proportional to the hydrogen production rate. The potential is decreased when the system temperature is increased at every current density.

For frequency and duty cycle, the hydrogen production rate is proportional to the duty cycle but is inversely proportional to the frequency because it relates to the peak and average power in the determination of total energy output. When considering the efficiency of the process, the efficiency is diminished when the duty cycle and frequency are increased because during the "on-time" period, the accumulation of gas bubbles is occurred on the electrodes, blocking the flow of electrical current. the pulsed current scheme provides higher efficiency than the continuous one. Hence the duty cycle and frequency influence the hydrogen production rate and efficiency of the electrolyzer.

The different of flowing electrolyte are compared to improve the efficiency of the electrolysis process. Gas bubble is formed and covers the electrode surface which is assumed as an additional electrical resistance to the system, leading to the low efficiency of the electrolysis process. The physical properties of the electrolyte related conductivity such as bubble layer at electrodes surface can be reduced by improving mass transport which is consisted in the electrical conductivity of the electrolyte.